Tunneling in a linear B_2H_6–HCl dimer

Carl Chuang, T. D. Klots, R. S. Ruoff, Tryggvi Emilsson, and H. S. Gutowsky
Noyes Chemical Laboratory, University of Illinois, Urbana, Illinois 61801

(Received 20 February 1991; accepted 23 April 1991)

Rotational spectra have been observed for eight isotopic species of the diborane–HCl complex with a Balle–Flygare, pulsed nozzle, Fourier transform microwave spectrometer. The dimer has a linear, or at most slightly bent B–B···H/DCl equilibrium structure with the H/D end of the HCl attracted symmetrically to a terminal BH_2 group of the diborane. Three B_2H_6–HCl species homonuclear in the boron were observed to tunnel while those with $^{10}B^{11}BH_6$ or DCl did not. The tunneling splits each rotational transition into two components of comparable intensity, separated by several MHz depending on J and K. The a–dipole transitions are characteristic of a prolate, very near symmetric top; only $K = 0$ and ± 1 transitions were found. Rotational constants are reported for all species. The $\overline{B}$, D_J, H, $(B\text{-}C)$, and D_{JK} constants determined for $^{11}B_2H_6$–$H^{35}Cl$ are for the A_1 tunneling state 1273.364(1) MHz, 5.56(5) kHz, 1.0(8) Hz, 5.3(2) MHz, and $-2.1(3)$ MHz; for the A_2 tunneling state 1273.856(1) MHz, 11.64(7) kHz, 33.1(9) Hz, 5.70(4) MHz, and $-3.21(5)$ MHz. The chlorine hyperfine structure gives the average torsional displacement of the H/DCl from the a axis to be 26.3° for the HCl complexes and 22.5° for the DCl. The torsional displacement of the B_2H_6 was found by an inertial analysis of the complexes with HCl. It is very anisotropic, being close to 0° in the ethylene plane and about 9° in the BH_2B bridging plane. It is suggested that in the tunneling the B_2H_6 reorients by 180° in the bridging plane, coupled with a gear-like counter rotation of the HCl by 360°. The B···H distance is 2.693 Å in the dimers with HCl and the $B\cdots D$ distance is slightly longer, 2.702 Å.

INTRODUCTION

Diborane is an unusual molecule with a bridging structure involving two three-center B–H–B bonds.[1] With the thought that this structure could lead to unusual van der Waals and hydrogen bonded complexes, the diborane–HF dimer was studied previously.[2] It was found to have a linear BB–HF equilibrium configuration with the H end of HF attracted symmetrically to one of the terminal BH_2 groups, in which the hydrogens are negative. In the present work, the diborane–HCl complex is studied. Although its equilibrium structure is basically linear like the HF counterpart, diborane–HCl undergoes tunneling which splits the rotational transitions of several of the isotropic species into two components.

The tunneling is a geared motion in which the HCl samples both terminal BH_2 groups of diborane. It is quenched when the two borons are not equivalent as in $^{10}B^{11}BH_6$–HCl and $^{11}B^{10}BH_6$–HCl and when DCl is substituted for HCl. Large internal mobility of diborane–HCl is indicated by the centrifugal distortion constants and by the strong isotopic dependence of the tunneling splittings and of the centrifugal distortion.

Tunneling in hydrogen bonded and van der Waals dimers has long been of experimental and theoretical interest. Typically the tunneling involves light atoms like hydrogen in monomers such as the hydrogen halides, water, or ammonia, the structures of which are preserved in the motions of the dimers. Molecules like HF dimer[3] and H_2O dimer[4] are prototypes in the understanding of these phenomena. Tunneling involving heavier atoms in the monomers has also been observed, e.g., in the SO_2 dimer.[5] A more recent example is the tunneling affecting all three monomers in the quasi-T-shaped trimer HCN–$(CO_2)_2$.[6]

Some of the tunneling mechanisms have been found to be quite complex. An interesting case is the acetylene dimer which undergoes interconversion tunneling between four equivalent hydrogen bonded T-shaped configurations.[7] The tunneling in N_2–H_2O (Ref. 8) is similar to that in diborane–HCl. In both cases it involves reorientational motions of the two monomers. The tunneling properties of diborane–HCl are presented in this paper. Also given are details of the rotational spectra for several isotopic species and the derivation from them of rotational constants, dimer geometry, and torsional motions of the monomers.

EXPERIMENT

Rotational spectra of the ground vibrational state were observed with a Balle–Flygare pulsed nozzle, Fourier transform microwave spectrometer.[9] The diborane–HCl dimer forms during expansion from the supersonic nozzle of the carrier gas seeded with diborane and HCl. It is hit with pulses of microwave radiation as it crosses the Fabry–Perot cavity. When the microwave frequency corresponds to a transition frequency of the dimer, the dimer is polarized. The resulting free induction decay (FID) is digitized and Fourier transformed to obtain the spectrum. Spectrometer operation and averaging are now handled by a personal computer based system.[10] Up to 16 FIDs can be recorded per gas pulse, which is repeated at a rate of up to 30 cps.

The gas mixture behind the 1.0 mm diam nozzle was adjusted with needle valves that set the flow rates of a 20% HCl or DCl in He mixture, of a 10% diborane in He mixture, and of Ar which was used as the carrier gas. Signal was optimized when the HCl or DCl and diborane were each approximately 1% of the final mixture. The pressure back-

 0021-9606/91/151552-11$03.00

ing the nozzle was regulated at 1 atm. Diborane was purchased from Matheson Gas. DCl was synthesized locally by adding D_2O to benzoyl chloride.

The search for transitions of the diborane–HCl dimers was guided by our previous results for diborane–H/DF.[2] By in large the main surprises it produced were the tunneling splittings of 1 to 3 MHz associated with the tunneling and a large negative D_{JK} centrifugal distortion. The large number of hyperfine interactions presented some problems however. The chlorine nuclear quadrupole coupling with a χ_0 of -67.619 and -53.294 MHz for free $H^{35}Cl$ and $H^{37}Cl$, respectively,[11] is larger by 20-fold or more than the others,[2] which include the boron quadrupole interactions and many small dipole–dipole interactions within the B_2H_6 and that in HCl. The net result is that the hyperfine structure (hfs) caused by χ_{aa}(Cl) is resolved in the observed transitions while the other interactions serve mainly to broaden the chlorine hf components. Usually, the signals were readily detected in spite of the broadening. The strongest transitions of $^{11}B_2H_6$–$H^{35}Cl$, the most abundant isotopic species, have hf components with a signal to noise ratio of about 10 for a single gas shot.

The quadrupole interactions of the two borons are larger than the various dipole–dipole terms and produce some

TABLE I. Observed and calculated frequencies of the chlorine hyperfine components for the rotational transitions of $^{11}B_2H_6$–$H^{35}Cl$ in the A_1 and A_2 tunneling states.[a]

		A_1		A_2	
$J,K,F \rightarrow J',K',F'$		Observed (MHz)	Obs − Calc (kHz)	Observed (MHz)	Obs − Calc (kHz)
0,0,3/2	1,0,3/2	2 537.17	b	2 538.15	b
3/2	5/2	2 549.10	b	2 550.06	b
3/2	1/2	2 558.644	0	2 559.606	0
1,0,1/2	2,0,3/2	5 081.372	2	5 083.163	1
5/2	5/2	5 082.379	−2	5 084.170	−2
1/2	1/2	5 093.277	0	5 095.063	2
5/2	7/2	5 094.302	0	5 096.085	−1
3/2	3/2	5 102.83	b	5 104.61	b
2,0,7/2	3,0,7/2	7 628.226	−1	7 630.578	1
3/2	5/2	7 637.185	−2	7 639.529	−3
7/2	9/2	7 640.153	3	7 642.494	2
5/2	5/2	7 645.727	−1	7 648.066	−1
3/2	3/2	7 649.10	b	7 651.43	b
3,0,5/2	4,0,7/2	10 184.460	2	10 187.045	−1
9/2	11/2	10 185.845	−2	10 188.434	1
4,0,7/2	5,0,9/2	12 730.266	1	12 732.803	1
11/2	13/2	12 731.088	−1	12 733.624	−1
4, −1,7/2	5, −1,9/2	12 736.05	23	12 743.80	30
9/2	11/2	12 736.56	−2	12 744.25	−17
5/2	7/2	12 736.60	−22	12 744.34	−26
11/2	13/2	12 737.16	1	12 744.88	14
4, +1,7/2	5, +1,9/2	12 761.31	−4	12 772.47	16
9/2	11/2	12 761.85	13	12 773.04	22
5/2	7/2	12 761.89	−18	12 773.04	−10
11/2	13/2	12 762.445	10	12 773.59	−28
5,0,9/2	6,0,11/2	15 275.154	0	15 277.405	−2
13/2	15/2	15 275.700	0	15 277.955	2
5, −1,9/2	6, −1,11/2	15 279.67	9	15 286.80	−8
7/2	9/2	15 279.98	−20	15 287.10	−48
11/2	13/2	15 280.07	−4	15 287.23	34
13/2	15/2	15 280.43	15	15 287.56	22
5, +1,9/2	6, +1,11/2	15 312.094	−10	15 320.79	−38
7/2	9/2	15 312.48	36	15 321.14	−28
11/2	13/2	15 312.48	−30	15 321.32	59
13/2	15/2	15 312.854	4	15 321.61	7

[a] The $K = 0$ transitions were fitted together for each state as were the $K = \pm 1$. The frequencies of the $K = \pm 1$ components were estimated. The line centers from the fits are included in Table V and the χ_{aa}'s in Tables VIII and IX for $K = 0$ and ± 1, respectively.

[b] Estimated, not included in the fit.

discernible splittings. However, the $K = 0$ transitions are affected only by χ_{aa}, which is the smallest element in the boron tensor, and the splittings by it are visible in only a few of the low J, $K = 0$ chlorine hf components, and were not used in the fitting. The line broadening from the various smaller interactions increases the standard deviation of frequency measurements for the $K = 0$ components to about $\pm$ 3 kHz. The $K = \pm 1$ components are split into broad and complicated patterns by the $(\chi_{bb} - \chi_{cc})$ elements of the two borons, which we estimate to be 2–3 MHz in magnitude. The splittings spread over 400 kHz in the $J = 1 \rightarrow 2$ transition and over 100 kHz in the $J = 5 \rightarrow 6$ transition. No effort was made to assign the patterns, and line centers were simply estimated. This gives relatively large uncertainties of about $\pm$ 50 kHz for the $K = \pm 1$ frequencies.

RESULTS AND ANALYSIS

Transitions, hfs, and assignments

The two stable isotopes of boron are ^{10}B (20%, $I = 3$, $Q = +0.074$) and ^{11}B (80%, $I = 3/2$, $Q = +0.036$). So diborane has the three isotopic species $^{11}B^{11}BH_6$ (64%), $^{11}B^{10}BH_6$ (32%), and $^{10}B^{10}BH_6$ (4%). Chlorine has two isotopes, ^{35}Cl (76%) and ^{37}Cl (24%), both of which have nuclear spins of 3/2. Accordingly, there are many isotopic variants of the diborane–H/DCl dimer. For simplicity we designate them in the text with an alphanumeric code based on the mass numbers of the isotopically substituted nuclei, e.g., $^{10}B^{11}BH_6$–$D^{35}Cl$ is 10,11-D35. Of the species available we have observed and assigned transitions and chlorine hfs for eight: 11,11–H35; 10,11–H35; 11,10–H35; 10,10–H35; 11,11–H37; 10,11–H37; 11,11–D35; and 10,11–D35. The results are presented in Tables I–IV.

Each isotopic species was observed to have a–dipole transitions characteristic of a prolate, very near symmetric top. The small values of $\sim$5 MHz found for $(B–C)$ require that the heavy atoms be linear, or nearly so.[2] This is supported by the presence of two isomers with the mixed $^{10}B^{11}BH_6$ diborane, the 10,11–H35 and 11,10–H35 species which show that the HCl is located at one or the other of the terminal BH_2 groups.

For the homonuclear boron species with HCl (11,11–H35; 11,11–H37; and 10,10–H35) all transitions were split into two sets of hf components (Tables I and II) with comparable intensity. The magnitudes of the splittings are only a few MHz and they vary depending on the rotational transition and isotopic species. No splittings were observed for the species that are heteronuclear with respect to the boron nuclei or for any dimer with DCl regardless of the isotopic makeup of the borons.

Only the $K = 0$ and $K = \pm 1$ transitions were found for each species. Presumably higher K states are too high in energy to be populated in the molecular beam. In all of the diborane–HCl species, for each $J \rightarrow J + 1$ both the $K = -1$ and $K = +1$ transitions are higher in frequency than the $K = 0$ transition. Typically, for prolate, near symmetric tops, the $K = 0$ transition lies between the $K = -1$ and $K = +1$ transitions. For the DCl complexes, however, the K = 0 transitions do lie between the K = −1 and K = +1 transitions. Assignment of the K states is based primarily on the chlorine hfs which differs greatly for $K = 0$ and $K = \pm 1$. It is confirmed by calculating the frequencies for $K = 0$ transitions at higher J from that for $J = 0 \rightarrow 1$ which is $\sim 2\overline{B}$.

The most extensive measurements ($J = 0 \rightarrow 1$ to $5 \rightarrow 6$) were made for 11,11–H35, the most abundant species. The hyperfine frequencies are given in Table I for both tunneling states, with the lower frequency line of each tunneling pair designed as the A_1 state and the higher as the A_2 state. Al-

TABLE II. Observed and calculated frequencies of the chlorine hyperfine components for the $K = 0$, $J = 3 \rightarrow 4$ to $5 \rightarrow 6$ rotational transitions of $^{11}B_2H_6$–$H^{37}Cl$ and $^{10}B_2H_6$–$H^{35}Cl$ in the A_1 and A_2 tunneling states.[a]

		A_1		A_2	
$J,K,F \rightarrow J',K',F'$		Observed (MHz)	Obs − Calc (kHz)	Observed (MHz)	Obs − Calc (kHz)
		$^{11}B_2H_6$–$H^{37}Cl$			
3,0,5/2	4,0,7/2	9 961.019	0	9 963.346	1
9/2	11/2	9 962.114	0	9 964.438	−1
4,0,7/2	5,0,9/2	12 450.883	1	12 453.179	0
11/2	13/2	12 451.531	−1	12 453.828	0
5,0,9/2	6,0,11/2	14 939.921	0	14 941.982	−1
13/2	15/2	14 940.352	0	14 942.413	1
		$^{10}B_2H_6$–$H^{35}Cl$			
3,0,5/2	4,0,7/2	10 632.720	0	10 637.447	0
9/2	11/2	10 634.099	−1	10 638.825	0
4,0,7/2	5,0,9/2	13 290.339	1	13 294.944	2
11/2	13/2	13 291.157	−1	13 295.758	−2
5,0,9/2	6,0,11/2	15 946.861	−4	15 950.924	−3
13/2	15/2	15 947.413	4	15 951.472	3

[a] The transitions were fitted together for each dimer and state. The line centers from the fits are included in Table V and the χ_{aa}'s in Table VIII.

TABLE III. Observed and calculated frequencies of the chlorine hyperfine components in the rotational transitions of $^{10}B^{11}BH_6$–$H^{35}Cl$ and $^{11}B_2H_6$–$D^{35}Cl$.[a]

		$^{10}B^{11}BH_6$–$H^{35}Cl$		$^{11}B_2H_6$–$D^{35}Cl$	
$J,K,F \rightarrow J',K',F'$		Observed (MHz)	Obs − Calc (kHz)	Observed (MHz)	Obs − Calc (kHz)
0,0,3/2	1,0,7/2	2 624.30	b		
3/2	5/2	2 636.20	b		
3/2	1/2	2 645.730	0		
1,0,1/2	2,0,3/2	5 255.471	2	5 061.898	0
5/2	5/2	5 256.48	b		
1/2	1/2	5 267.363	− 3	5 074.993	1
5/2	7/2	5 268.391	1	5 076.119	− 1
3/2	3/2	5 276.90	b		
2,0,7/2	3,0,7/2	7 889.10	b		
3/2	5/2	7 898.04	− 5		
7/2	9/2	7 901.005	1		
5/2	5/2	7 906.580	4		
3/2	3/2	7 909.92	b		
2, − 1,7/2	3, − 1,7/2	7 904.3	12		
5/2	7/2	7 910.0	− 54		
7/2	9/2	7 913.0	− 20		
5/2	5/2	7 914.2	62		
2, + 1,7/2	3, + 1,7/2	7 919.8	25		
5/2	7/2	7 925.8	− 16		
7/2	9/2	7 928.7	− 81		
5/2	5/2	7 930.1	72		
3,0,5/2	4,0,7/2	10 531.824	1	10 148.243	− 1
9/2	11/2	10 533.211	2	10 149.771	0
7/2	7/2	10 537.394	− 3	10 154.382	0
4,0,7/2	5,0,9/2	13 163.869	4	12 685.512	2
11/2	13/2	13 164.685	− 4	12 686.416	− 2
4, − 1,7/2	5, − 1,9/2	13 176.35	57	12 673.21	25
9/2	11/2	13 176.76	− 50	12 673.77	18
5/2	7/2	13 176.90	16	12 673.77	− 61
11/2	13/2	13 177.38	− 24	12 674.42	18
4, + 1,7/2	5, + 1,9/2	13 204.47	− 61	12 704.16	− 4
9/2	11/2	13 205.07	4	12 704.77	22
5/2	7/2	13 205.16	38	12 704.77	− 40
11/2	11/2	13 205.68	20	12 705.42	22
5,0,9/2	6,0,11/2	15 794.730	0	15 222.128	0
13/2	15/2	15 795.275	0	15 222.729	0
5, − 1,9/2	6, − 1,11/2	15 806.02	39	15 207.36	− 5
7/2	9/2	15 806.33	12	15 207.77	36
11/2	13/2	15 806.41	29	15 207.77	− 36
13/2	15/2	15 806.64	− 80	15 208.18	4
5, + 1,9/2	6, + 1,11/2	15 840.67	18	15 244.57	− 2
7/2	9/2	15 840.96	− 29	15 244.99	49
11/2	13/2	15 841.06	− 5	15 244.99	− 32
13/2	15/2	15 841.42	16	15 245.38	− 14

[a] The $K = 0$ transitions were fitted together for each dimer as were the $K = \pm 1$. The frequencies of the $K = \pm 1$ components were estimated. The line centers from the fits are included in Table VI and the χ_{aa}'s in Tables VII and IX for $K = 0$ and ± 1, respectively.

[b] Estimated, not included in the fit.

though $K = \pm 1$ transitions were observed from $J = 1 \rightarrow 2$ to $J = 5 \rightarrow 6$, only the $J = 4 \rightarrow 5$ and $J = 5 \rightarrow 6$ are reported. The chlorine hf components for the low $J,K = \pm 1$ transitions are too severely complicated by the boron hfs to estimate line centers. Also many lines are overlapped due to the splittings.

Only $K = 0$ transitions were observed for 11,11–H37 and 10,10–H35. The hfs of both the A_1 and A_2 states is re-

TABLE IV. Observed and calculated frequencies of the chlorine hyperfine components for the $K=0$, $J=3\rightarrow4$ to $5\rightarrow6$ rotational transitions of $^{10}B^{11}BH_6$–$H^{37}Cl$, $^{11}B^{10}BH_6$–$H^{35}Cl$, and $^{10}B^{11}BH_6$–$D^{35}Cl$.[a]

$J,K,F\rightarrow J',K',F'$		Observed (MHz)	Obs − Calc (kHz)	Observed (MHz)	Obs − Calc (kHz)
		$^{10}B^{11}BH_6$–$H^{37}Cl$		$^{11}B^{10}BH_6$–$H^{35}Cl$	
3,0,5/2	4,0,7/2	10 305.187	− 1	10 276.450	− 2
9/2	11/2	10 306.280	1	10 277.840	2
4,0,7/2	5,0,9/2	12 880.547	1	12 844.690	3
11/2	13/2	12 881.192	− 1	12 845.507	− 3
5,0,9/2	6,0,11/2	15 454.844	0	15 411.777	− 1
13/2	15/2	15 455.274	0	15 412.320	− 1
		$^{10}B^{11}BH_6$–$D^{35}Cl$			
3,0,5/2	4,0,7/2	10 492.810	− 1		
9/2	11/2	10 494.344	1		
4,0,7/2	5,0,9/2	13 116.174	4		
11/2	13/2	13 117.077	− 4		
5,0,9/2	6,0,11/2	15 738.842	− 4		
13/2	15/2	15 739.452	4		

[a] The line centers from the fits are included in Table VII and the χ_{aa}'s in Table VIII.

ported for $J=3\rightarrow4$ to $5\rightarrow6$ in Table II. More extensive observations, including $K=\pm1$ transitions, were made for 10,11–H35 and 11,11–D35. The results are given in Table III. As with 11,11–H35 the $K=\pm1$ chlorine hfs components were complicated by boron hfs, so the estimated line centers have uncertainties of ± 50 kHz. Only $K=0$ transitions were observed for 10,11–H37, 11,10–H37, and 10,11–D35. The frequencies of the hf components are given in Table IV for $J=3\rightarrow4$ to $5\rightarrow6$.

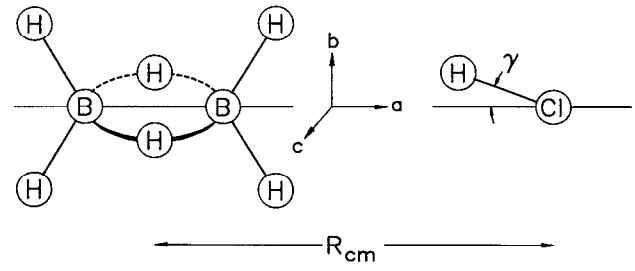

FIG. 1. Geometrical structure and inertial axes of the diborane–HCl dimer. The atomic positions are drawn to scale; γ is the angle in three dimensions between the HCl and a axes.

Comparison of signal strengths revealed that the 10,11–H35 species is about twice as strong as the 11,10–H35. A similar observation was made between 10,11–HF and 11,10–HF.[2] The difference in the abundance of the two species is probably caused by the higher zero-point energy of the 11,10–HCl species.

Analysis of hfs to obtain χ_{aa}(Cl) and line centers

The observed hfs given in Tables I–IV was fitted to determine the chlorine quadrupole interaction constants and the line centers for the transitions. The inertial axes and dimer geometry employed are given in Fig. 1. The Hamiltonian used in the analysis consisted of rotational and chlorine

TABLE V. Observed and calculated line centers for rotational transitions of the dimers with A_1 and A_2 tunneling states:[a] $^{11}B_2H_6$–$H^{35}Cl$, $^{11}B_2H_6$–$H^{37}Cl$, and $^{10}B_2H_6$–$H^{35}Cl$.

Transition $J,K\rightarrow J',K'$		A_1 Observed (MHz)	A_1 Obs − Calc (kHz)	A_2 Observed (MHz)	A_2 Obs − Calc (kHz)	$\Delta\nu$ (MHz)
			$^{11}B_2H_6$–$H^{35}Cl$			
0,0	1,0	2 546.700	− 5	2 547.670	5	0.970
1,0	2,0	5 093.277	1	5 095.061	3	1.784
2,0	3,0	7 639.580	0	7 641.923	− 5	1.343
3,0	4,0	10 185.484	4	10 188.071	− 3	2.587
4,0	5,0	12 730.835	− 4	12 733.371	5	2.536
4, − 1	5, − 1	12 736.712	517	12 744.429	− 105	7.717
4, + 1	5, + 1	12 761.991	− 517	12 773.160	105	11.169
5,0	6,0	15 275.517	1	15 277.769	− 1	2.247
5, − 1	6, − 1	15 280.112	− 431	15 287.243	88	7.131
5, + 1	6, + 1	15 312.551	431	15 321.293	− 88	8.742
			$^{11}B_2H_6$–$H^{37}Cl$			
3,0	4,0	9 961.828	b	9 964.153	b	2.325
4,0	5,0	12 451.332		12 453.628		2.296
5,0	6,0	14 940.207		14 942.268		2.061
			$^{10}B_2H_6$–$H^{35}Cl$			
3,0	4,0	10 633.739	b	10 638.465	b	4.726
4,0	5,0	13 290.905		13 295.507		4.602
5,0	6,0	15 947.226		15 951.287		4.061

[a] The "observed" line centers are from the fits of the hfs in Tables I and II. The residues for 11,11–H35 are from separate fits for the $K=0$ and $K=\pm1$ states.
[b] Data insufficient to give residues.

TABLE VI. Observed and calculated line centers for rotational transitions of $^{10}B^{11}BH_6$–$H^{35}Cl$ and $^{11}B_2H_6$–$D^{35}Cl$.[a]

Transition $J,K \rightarrow J',K'$	$^{10}B^{11}BH_6$–$H^{35}Cl$ Observed (MHz)	Obs − Calc[b] (kHz)	$^{11}B_2H_6$–$D^{35}Cl$ Observed (MHz)	Obs − Calc[b] (kHz)
0,0 1,0	2 633.798	− 3		
1,0 2,0	5 267.366	8	5 074.992	− 1
2,0 3,0	7 900.435	− 5		
2, − 1 3, − 1	7 911.756	880		
2, + 1 3, + 1	7 927.504	− 364		
3,0 4,0	10 532.848	− 2	10 149.372	2
4,0 5,0	13 164.435	3	12 686.137	− 1
4, − 1 5, − 1	13 176.963	− 338	12 673.920	6
4, + 1 5, + 1	13 205.215	− 414	12 704.910	− 6
5,0 6,0	15 795.092	− 1	15 222.527	0
5, − 1 6, − 1	15 806.422	− 158	15 207.850	− 6
5, + 1 6, + 1	15 841.102	529	15 245.064	6

[a] The "observed" line centers are from the fits of the hfs in Table III.
[b] The residues are from separate fits for the $K = 0$ and $K = \pm 1$ states.

nuclear quadrupole interaction terms:

$$H = H_r + H_q(\mathrm{Cl}). \tag{1}$$

Spin–rotation interactions, the H/DCl and intra-B_2H_6 dipole interactions, the deuterium quadrupole interaction, and the χ_{aa} quadrupole elements for the two boron nuclei are small and were neglected. The $(\chi_{bb} - \chi_{cc})$ interactions of the two borons were also ignored although they had considerable effect on $K = \pm 1$ lines. The splittings by them were too complicated and not sufficiently resolved to attempt assignment.

One would expect the torsional oscillations of HCl and DCl to be anisotropic so that the chlorine $(\chi_{bb} - \chi_{cc})$ interaction is nonzero. However, the frequencies of the $K = \pm 1$ chlorine hyperfine components were not accurate enough because of congestion by the boron hfs for $(\chi_{bb} - \chi_{cc})$ to be determined. Nevertheless, the anisotropy is small, < 1 MHz, compared with χ_{aa} so $(\chi_{bb} - \chi_{cc})$ was fixed at 0 for the chlorine in the fitting.

Thus the only hyperfine interaction considered was χ_{aa} for chlorine. Matrix elements were calculated in the coupled basis set $F = J + I$, where $I = 3/2$ for both chlorine isotopes. Matrix blocks of F were diagonalized to get hyperfine energies. The hfs was fitted for each species using χ_{aa} and the line centers as adjustable parameters. The $K = 0$ hyperfine components were much more precisely determined, so they were fitted separately from the $K = \pm 1$. The residuals of the fits are included in Tables I–IV. The unperturbed line centers obtained from fitting the hfs are listed in Tables V–VII. The values determined for χ_{aa}(Cl) from the $K = 0$ hfs are given for all isotopic species and their tunneling states in Table VIII while those from $K = \pm 1$ hfs are given in Table IX.

TABLE VII. Observed line centers for rotational transitions of $^{10}B^{11}BH_6$–$H^{37}Cl$, $^{11}B^{10}BH_6$–$H^{35}Cl$, and $^{10}B^{11}BH_6$–$D^{35}Cl$.[a]

Transition $J,K \rightarrow J',K'$	$^{10}B^{11}BH_6$–$H^{37}Cl$ (MHz)	$^{11}B^{10}BH_6$–$H^{35}Cl$ (MHz)	$^{10}B^{11}BH_6$–$D^{35}Cl$ (MHz)
3,0 4,0	10 305.994	10 277.476	10 493.943
4,0 5,0	12 880.994	12 845.256	13 116.799
5,0 6,0	15 455.129	15 412.138	15 739.246

[a] The "observed" line centers are from the fits of the hfs in Table IV.

Determination of rotational constants

The $K = 0$ line centers were fitted to the equation for a distortable, nearly linear rotor:[12]

$$H_r = \overline{B}J(J+1) - D_J[J(J+1)]^2 + H[J(J+1)]^3, \tag{2}$$

where $\overline{B} = (B + C)/2$. The residues of the fit are included in Tables V and VI. The fitted values for $\overline{B}$, D_J, and H are given in Table VIII. For those species where only three line centers, $J = 3 \rightarrow 4$ to $5 \rightarrow 6$, were determined, the fit is exact so residues and standard deviations are missing.

The $K = \pm 1$ transitions were fitted separately using the equation for a distortable, prolate, near-symmetric top:[12]

$$H_r = AJ_g^2 + BJ_g^2 + CJ_g^2 - D_J[J^2(J+1)^2] - D_{JK}J(J+1)J_g^2. \tag{3}$$

B and C were constrained so that their average equals $\overline{B}$ as determined from the $K = 0$ fit. The fits of the $K = \pm 1$ transitions were insensitive to A since $(B - C)$ is small and A is large, predicted at about 70 GHz compared with 80 GHz found for free diborane.[1] The residues of the fits are included in Tables V and VI. As can be seen, those for 11,11–H35 and 10,11–H35 are quite large, several hundred kHz, suggesting higher order distortion constants are necessary. The fitted values of $(B - C)$, D_J, and D_{JK} are given in Table IX.

The line centers identified with the A_1 and A_2 tunneling states were fitted separately, giving the rotational constants in Tables VIII and IX. In the case of 11,11–H35, for which we have the most data, the quality of the fit is the same for both states and that for the $K = 0$ transitions is comparable with that for the diborane–HF dimer. This supports our assumption that the observed splittings do not involve transi-

TABLE VIII. Spectroscopic constants determined from the $K = 0$ transitions of several isotopic species of the diborane–HCl dimer.[a]

Species	$\overline{B}$ (MHz)	D_J (kHz)	H (Hz)	χ_{aa}(Cl) (MHz)	γ (deg)
$^{11}B_2H_6$–$H^{35}Cl$ (A_1)	1 273.364(1)	5.56(5)	1.0(8)	−47.701(5)	26.30
(A_2)	1 273.856(1)	11.64(7)	33.1(9)	−47.670(6)	26.33
$^{11}B_2H_6$–$H^{37}Cl$ (A_1)	1 245.399	5.34	0.8	−37.641(31)	26.26
(A_2)	1 245.828	10.31	26.2	−37.586(30)	26.31
$^{10}B_2H_6$–$H^{35}Cl$ (A_1)	1 329.443	7.06	0.1	−47.473(182)	26.47
(A_2)	1 330.335	17.86	57.3	−47.361(143)	26.55
$^{10}B^{11}BH_6$–$H^{35}Cl$	1 316.921(2)	10.36(8)	20.9(11)	−47.657(13)	26.34
$^{10}B^{11}BH_6$–$H^{37}Cl$	1 288.536	9.37	16.9	−37.542(59)	26.35
$^{11}B^{10}BH_6$–$H^{35}Cl$	1 284.991	10.09	20.4	−47.622(148)	26.36
$^{11}B_2H_6$–$D^{35}Cl$	1 268.774(1)	3.22(3)	0.4(5)	−52.465(6)	22.60
$^{10}B^{11}BH_6$–$D^{35}Cl$	1 311.856	3.58	1.4	−52.652(206)	22.45

[a] χ_0(Cl) has been determined to be −67.6189, −53.294, and −67.3934 MHz, respectively, in free $H^{35}Cl$, $H^{37}Cl$, and $D^{35}Cl$ (Ref. 11).

tions between two different tunneling states, but are due instead to slightly different rotational constants for the two tunneling states.

Dimer geometry

Figure 1 gives the geometrical structure indicated for B_2H_6–HCl by the data obtained. It has a linear or near linear heavy atom backbone with the H end of the HCl closest to one of the terminal BH_2 groups. This is the same as the HF counterpart[2] and the evidence for it is similar. If we neglect the relatively small effects of torsional oscillations of the monomers, one finds with the parallel axis theorem[13] that I_{bb} and I_{cc} of the linear dimer are given by

$$I_{gg}(\text{dimer}) = I_g(B_2H_6) + I_o(\text{H/DCl}) + \mu_d R^2, \qquad (4)$$

where $g = b$, c, and $I_g(B_2H_6)$ and I(H/DCl) are the moments of inertia for the monomers, μ_d is the reduced mass of the dimer treated as pseudodiatomic, and R is the center of mass (c.m.) to c.m. separation of the monomers.

Equation (4) was used to calculated R for 11,11–H35(A_1) and 11,11–D35 using the experimental rotational constants in Tables VIII and IX and those reported for the monomers.[1,11] If the H end of HCl is closest to the boron, substitution of D in it with no change in structure moves the DCl c.m. 0.034 Å closer to the boron (shortens R). But if the Cl is closest to the boron, D substitution lengthens R by the same amount. We find that R is 0.029 Å shorter in 11,11–D35 than in 11,11–H35(A_1), supporting the BB–H/DCl orientation. The difference is a bit smaller than predicted, mainly because the torsional oscillations were neglected.

Evidence for the linearity of the dimer is also provided by Eq. (4) which predicts that for a linear dimer

$$(I_c - I_b)(\text{dimer}) = (I_c - I_b)(B_2H_6). \qquad (5)$$

This prediction is tested in Table X which lists the values of I_b, I_c, and $(I_c - I_b)$ determined for $^{11}B_2H_6$ and $^{10}B^{11}BH_6$ and for the four species of dimer for which values of both $\overline{B}$ and $(B - C)$ were obtained. It is seen that $(I_c - I_b)$ is virtually the same, 2.455 μÅ^2, for both species of diborane as it should be. However, in the dimer $(I_c - I_b)$ is visibly smaller, $\sim$1.75 μÅ^2. In principle the decrease could be caused either by a bent equilibrium structure or by anisotropic bending oscillations of the diborane in a linear dimer. The methods employed in the following section show that a bent structure with the diborane rotated by $\sim 10°$ about its b axis will fit a value of 1.75 μÅ^2 for $(I_c - I_b)$ in the dimer. However, anisotropic oscillation of the diborane seems more likely.

Bending vibrations of HCl and B_2H_6

The bending vibrations of HCl and B_2H_6 in the dimer are large enough to produce readily visible effects in spite of

TABLE IX. Spectroscopic constants determined from the $K = \pm 1$ transition of $^{11}B_2H_6$–$H^{35}Cl$ (A_1 and A_2), $^{10}B^{11}BH_6$–$H^{35}Cl$, and $^{11}B_2H_6$–$D^{35}Cl$.[a]

Species	$(B - C)$ (MHz)	D_{JK} (MHz)	D_J (kHz)	χ_{aa}(Cl) (MHz)	γ (deg)
$^{11}B_2H_6$–$H^{35}Cl$ (A_1)	5.3(2)	−2.1(3)	11(4)	−47.602(754)	26.4
(A_2)	5.70(4)	−3.21(5)	23.8(8)	−47.737(1.287)	26.3
$^{10}B^{11}BH_6$–$H^{35}Cl$	5.7(1)	−3.40(10)	23(2)	−47.339(221)	26.6
$^{11}B_2H_6$–$D^{35}Cl$	6.201(3)	−0.327(3)	3.18(5)	−51.794(1.295)	23.1

[a] In the analysis, $\overline{B}$ was constrained to the values given in Table VIII, obtained by fitting the $K = 0$ transitions.

TABLE X. Comparison of $(I_c - I_b)$[a] observed for $^{11}B_2H_6$[b] and $^{10}B^{11}BH_6$[c] with values found for several B_2H_6–H/DCl dimers.[d]

Species	I_b	I_c	$(I_c - I_b)$
$^{11}B_2H_6$	27.7941	30.2502	2.4561
$^{10}B^{11}BH_6$	26.9927	29.4473	2.4546
$^{11}B_2H_6$–$H^{35}Cl$ (A_1)	396.0608	397.7127	1.6519
(A_2)	395.8461	397.6213	1.7752
$^{10}B^{11}BH_6$–$H^{35}Cl$	382.9294	384.5904	1.6610
$^{11}B_2H_6$–$D^{35}Cl$	397.3499	399.2964	1.9465

[a] In units of $\mu Å^2$.
[b] The I's are from Ref. 1; the value for I_a ($^{11}B_2H_6$) is 6.3478.
[c] Calculated with the molecular geometry given in Ref. 1 for $^{11}B_2H_6$.
[d] From rotational constants given in Tables VIII and IX.

the unresolved hfs. In the case of HCl the observed chlorine quadrupole interaction $\chi_{aa}(\mathrm{Cl})$ can be used to determine the angle γ between the HCl bond axis and the a axis. It is found from the relation[14]

$$\chi_{aa}(\mathrm{Cl}) = (1/2)\chi_o(\mathrm{Cl})\langle 3\cos^2\gamma - 1\rangle, \tag{6}$$

where $\chi_o(\mathrm{Cl})$ is the quadrupole coupling constant of free HCl and the brackets indicate an average over the bending vibrations. This assumes that the electrical properties of HCl are unperturbed by dimer formation. For a linear BB–HCl equilibrium geometry, γ represents the average torsional angle of HCl. Table VIII includes the γ's found from our $\chi_{aa}(\mathrm{Cl})$ results in the table by using the reported values of $\chi_o(\mathrm{Cl})$.[11] The γ's for HCl in the various isotopic dimers fall within a 0.3° range about the average of 26.35°. For dimers with DCl, γ is smaller, 22.5°, by an amount consistent with its two-fold larger moment of inertia.[15]

If the torsional oscillations of H/DCl are isotropic about the a axis, with an average amplitude of θ, its moment of inertia projects onto the a axis as $I_o(\mathrm{H/DCl})\ (1/2)\langle 1 + \cos^2\theta\rangle$.[14] The value of θ can be approximated by using the γ determined from the chlorine hyperfine interaction in Eq. (6), giving

$$I_b(\mathrm{H/DCl}) = I_c(\mathrm{H/DCl}) \simeq I_o(\mathrm{H/DCl})(1/2)\langle 1 + \cos^2\gamma\rangle. \tag{7}$$

The bending vibrations of diborane can be described by two angles θ_b and θ_c, which are angular displacements of the B–B axis with respect to principal inertial axes fixed in the linear dimer (Fig. 1). The bending is about the diborane c.m. with θ_b and θ_c in the ab and ac planes, respectively, of the dimer. Matrix methods[16] show that after such rotations the moments I'_g of the diborane in the fixed coordinate system are given by

$$I'_b = I_a\sin^2\theta_b + I_b\cos^2\theta_b,$$
$$I'_c = I_a\sin^2\theta_c + I_c\cos^2\theta_c, \tag{8}$$

where

I_a, I_b, and I_c are the principal moments of free diborane.

Equations (8) can be averaged over the torsional oscillations of the diborane and the results combined by means of the parallel axis theorem[13] with Eq. (7) for an oscillating HCl. This gives the following equations for I_b and I_c of the dimer with the diborane and HCl monomers oscillating about a linear equilibrium configuration:

$$I_{bb}(\mathrm{dimer}) = I_a(B_2H_6)\langle\sin^2\theta_b\rangle + I_b(B_2H_6)\langle\cos^2\theta_b\rangle + I_o(\mathrm{H/DCl})(1/2)\langle 1 + \cos^2\gamma\rangle + \mu_d R^2, \tag{9a}$$

$$I_{cc}(\mathrm{dimer}) = I_a(B_2H_6)\langle\sin^2\theta_c\rangle + I_c(B_2H_6)\langle\cos^2\theta_c\rangle + I_o(\mathrm{H/DCl})(1/2)\langle 1 + \cos^2\gamma\rangle + \mu_d R^2. \tag{9b}$$

Here, $\langle\sin^2\theta_g\rangle$ and $\langle\cos^2\theta_g\rangle$ are averages over the torsional oscillations.

For a rigid, linear structure, Eq. (9) reduces to Eq. (5) for the difference in moments, $(I_c - I_b)$ (dimer). Moreover it predicts that a rigid structure bent by θ_c in the ac plane would have

$$(I_{cc} - I_{bb})(\mathrm{dimer}) = I_a(B_2H_6)\sin^2\theta_c + I_c(B_2H_6)\cos^2\theta_c - I_b(B_2H_6). \tag{10}$$

Application of this result to the values of $(I_c - I_b)$ (dimer) in Table X leads to a bend angle θ_c of $\sim 10°$ as mentioned in the previous section. However, a bend in the ab plane will not fit the data.

In the case of an oscillating B_2H_6, Eq. (9) gives

$$(I_{cc} - I_{bb})(\mathrm{dimer}) = I_a(B_2H_6)\{\langle\sin^2\theta_c\rangle - \langle\sin^2\theta_b\rangle\} + I_c(B_2H_6)\langle\cos^2\theta_c\rangle - I_b(B_2H_6)\langle\cos^2\theta_b\rangle. \tag{11}$$

From the values of I_g given for diborane in Table X, we note that the terms in $I_a(B_2H_6)\langle\sin^2\theta_g\rangle$ are small so the value of $(I_{cc} - I_{bb})$ (dimer) is dominated in Eq. (11) by the terms in $\langle\cos^2\theta_g\rangle$. Moreover, θ_c must be significantly larger than θ_b to fit the finding in Table X that the observed $(I_{cc} - I_{bb})$ (dimer) is significantly smaller than $(I_c - I_b)(B_2H_6)$.

If we take the value of γ from $\chi_{aa}(\mathrm{HCl})$, Eq. (9) has three unknowns (θ_b, θ_c, and R) and only two observed quantities [I_{bb},I_{cc} (dimer)]. Also, the values of $(B - C)$ are not very precise, nor do we have very many of them (Table IX). The results found for both $\overline{B}$ and $(B - C)$ are given in Tables VIII and IX for 11,11–H35 and 10,11–H35. The B and C values obtained from them were fitted by Eq. (11). The 11,11–H35 dimer was taken as the parent with a c.m. to

TABLE XI. Results of fitting θ_c and R to the observed B and C values[a] for both $^{11}B^{11}BH_6$–$H^{35}Cl$,[b] and $^{10}B^{11}BH_6$–$H^{35}Cl$ at fixed values of θ_b.

θ_b (deg)	θ_c (deg)	R[c] (Å)	rms dev (MHz)
0	10.18	4.8222	0.104
1	10.22	4.8222	0.105
2	10.35	4.8224	0.106
4	10.86	4.8228	0.115
6	11.65	4.8236	0.141
8	12.68	4.8246	0.190
10	13.89	4.8259	0.263

[a] From Tables VIII and IX.
[b] The A_2 tunneling state was used in this fit.
[c] The R is that for 11,11–H35.

c.m. distance R_p, while that in 10,11–H35 was defined as $R_p - \Delta_i$ where Δ_i is a correction calculated for the isotopic shift in the c.m. of $^{10}B^{11}BH_6$ including the effects of its torsion. The fitting was done at fixed values of θ_b with θ_c and R as adjustable parameters. The findings are given in Table XI for θ_b ranging from 0° to 10°, using the B and C for the A_2 state of 11,11–H35.

It is seen that the rms deviation of the fit is smallest for $\theta_b = 0°$ and increases parabolically for larger θ_b. Moreover, both θ_c and R increase somewhat with θ_b, the increase of R being quite small. At the minimum deviation, with θ_b fixed at 0°, the fitted values of θ_c and R are 10.2° and 4.8222 Å, respectively. Although θ_b at 0° gives the best fit, it is unlikely that there is no torsion in the *ab* plane. The results should be interpreted as θ_b being close to zero. Also, the values of B and C for 11,11–D35 and of $\overline{B}$ for 10,11–D35 can be solved for θ_b, θ_c, and R, the results of which are 4.2°, 9.31°, and 4.8255 Å, respectively (referenced to 11,11–D35).

Structure information can also be obtained by fitting the experimental $\overline{B}$ which we have for all of the isotopic species (Table VIII). They are given by

$$\overline{B} = (505\,379.1/2)[(1/I_{bb}) + (1/I_{cc})], \qquad (12)$$

which can be combined with Eq. (9) to calculate $\overline{B}$ from θ_b,θ_c, and R for the various species. As before, the 11,11–H35 species was taken as the parent and isotopic shifts in c.m. were included in the fitting. This type of fit does not adequately constrain the *relative* values of B and C. So we held θ_b fixed at 0° as found in Table XI and adjusted only θ_c and R.

This approach gave best-fit values of 9.4° and 4.8219 Å for five of the species with HCl. The A_2 state was used for the tunneling species. The 10,10–H35 species was excluded because its spectroscopic parameters differ markedly from those for the other species (Table VIII) and its inclusion increases the rms deviation substantially. The value found for θ_c is somewhat smaller than that from B and C (9.4° vs 10.2°) and is probably more accurate. The results for R of 11,11–H35 are essentially identical.

With the average torsional angles θ_b,θ_c, and γ in hand for the B_2H_6 and H/DCl in the dimers we can use Eqs. (9) and (12) to determine R for each isotopic species from the $\overline{B}$ observed for it. The results are shown in Table XII which includes the angles found earlier. The R's are not directly comparable because of the shifts in c.m. with isotopic substitution. Therefore, they have also been converted to the isotopically independent distance between the boron and the H of the HCl, $r(B\cdots H)$. For the five dimers with HCl, $r(B\cdots H)$ varies by only 0.001 Å. The results for 11,11–D35 indicate that the deuterium substitution increases $r(B\cdots D)$ by 0.009 Å.

TABLE XII. Torsionally averaged structure parameters determined for various isotopic species of B_2H_6–H/DCl.

Species	θ_b (deg)	θ_c (deg)	γ (deg)	R[a] (Å)	$R(B\cdots H)$ (Å)
$^{11}B_2H_6$–$H^{35}Cl$ (A_2)	0	9.4	26.3	4.8219	2.6930
$^{11}B_2H_6$–$H^{37}Cl$ (A_2)	0	9.4	26.3	4.8237	2.6929
$^{10}B^{11}BH_6$–$H^{35}Cl$	0	9.4	26.3	4.7899	2.6934
$^{10}B^{11}BH_6$–$H^{37}Cl$	0	9.4	26.4	4.7916	2.6932
$^{11}B^{10}BH_6$–$H^{35}Cl$	0	9.4	26.4	4.8539	2.6926
$^{11}B_2H_6$–$D^{35}Cl$	4.2	9.3	22.6	4.7944	2.7019

[a] The values given include the isotopic shifts in monomer c.m.

Interaction potential

Information about the interaction potential forming the dimer can be derived from the D_J centrifugal distortion constant. We take the same approach as in the diborane–HF paper,[2] using a relationship between D_J and k_s which takes into account the inertial properties of the subunits[14]

$$D_J = 8\pi(\mu_d R_m)^2[(B^2 + C^2)^2 + 2(B^4 + C^4)]^{1/2}/\hbar k_s. \qquad (13)$$

We used this equation to estimate k_s and then calculated the well depth ϵ via the standard Lennard-Jones approach. The results are given in Table XIII.

Tunneling

Although the study of the diborane–HCl complex was undertaken as an extension of the diborane–HF work, it has turned out that the dimer with HCl is much different from its HF counterpart. Although both are linear in the equilibrium configuration, the potential surface of the HCl complex allows the monomers much more leeway to bend away from linearity. This is evident from the tunneling observed in the diborane–HCl complexes and from their large centrifugal distortion constants which are likely due to wide amplitude bending motions. Also the very large D_{JK} constants in the HCl complexes imply that there is considerable distortion upon excitation from the $K = 0$ state to the $K = \pm 1$ states

TABLE XIII. Effective potential constants approximated from D_J for various isotopic species of B_2H_6–H/DCl.

Species	k_s (mdyne/Å)	ν_s (cm^{-1})	ϵ (cm^{-1})
$^{11}B_2H_6$–$H^{35}Cl$ (A_1)	0.014 2	39	226
(A_2)	0.006 78	27	107
$^{10}B^{11}BH_6$–$H^{35}Cl$	0.008 25	30	128
$^{11}B_2H_6$–$D^{35}Cl$	0.024 4	50	386

and that the potential minimum at the linear configuration is not very steep.

The role of diborane in the tunneling is more readily apparent than that of the HCl. Splittings occur for all three B_2H_6–HCl dimers homonuclear in the boron but none were found in the heteroboron species (Tables V and VIII). This shows that the tunneling interchanges the two ends of the diborane molecule. It cannot be simply an inversion of a bent form because that would also occur for the heteroboron dimers. The direction in which the B_2H_6 rotates to interchange ends is evident in the marked anisotropy of its torsional oscillations. Clearly the B_2H_6 reorients much more easily about its b axis than the c axis. This path must have a lower barrier as well as less inertial resistance. Tunneling reorientation of the B_2H_6 is supported by the splittings given in Tables V and VIII. Those for the 10,10–H35 dimer are nearly double the splittings in the heavier 11,11–H35.

The participation of HCl in the tunneling appears to be a case of all or nothing. Substitution of ^{37}Cl for ^{35}Cl in 11,11–H35 reduces the splittings by only about 10%. On the other hand, substitution of D for H in the same dimer quenches the tunneling. No resolvable splittings were found in 11,11–D35 (Table VI). These results show that the HCl is an active participant in the tunneling, not a passive spectator. Reorientation of the HCl seems to be its most likely contribution to the tunneling. Substitution of ^{37}Cl increases I_o of $H^{35}Cl$ by only 0.002 $\mu Å^2$ from 1.615 (Ref. 11) but it decreases the splittings by 10%. However, substitution of D increases I_o to 3.126 $\mu Å^2$, nearly double that of $H^{35}Cl$. So it could well quench reorientation of the HCl and prevent the tunneling.

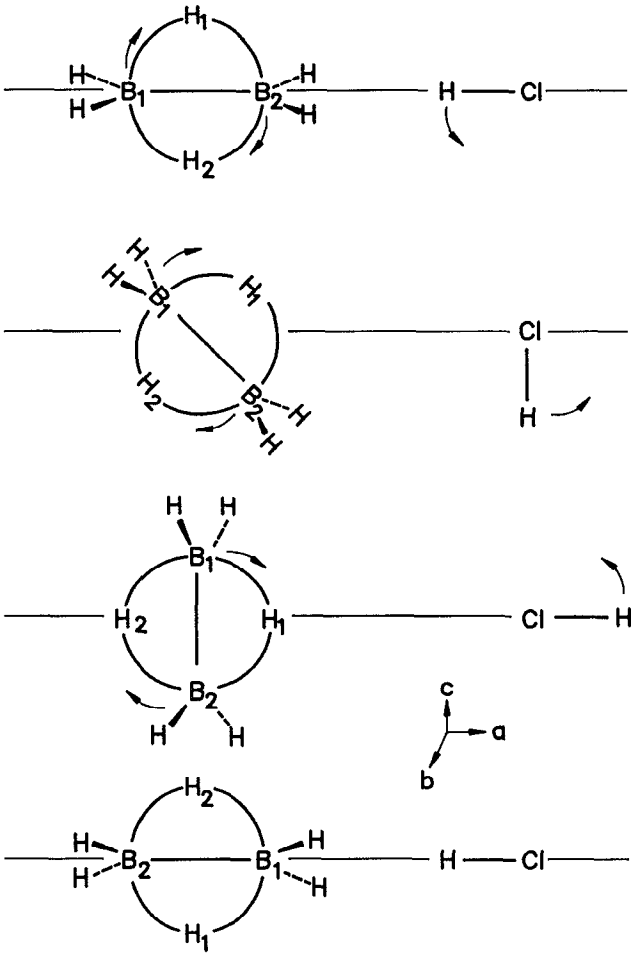

FIG. 2. Tunneling mechanism postulated for the homonuclear diborane–HCl isotopic species. The c.m.'s of the monomers are held fixed. The motion of the HCl is not as evident as that of the diborane.

DISCUSSION

The effects of isotopic substitution on tunneling in B_2H_6–HCl lead us to suggest that there must be strong coupling of the HCl reorientation with that of B_2H_6. Otherwise D substitution could quench the HCl reorientation but have little effect on tunneling of the B_2H_6. The splittings would then be reduced but not necessarily eliminated. The answer may be a concerted, gear-like motion as shown schematically in Fig. 2. Both monomers rotate about axes parallel to the b axis, in opposite directions, the HCl by 360° while the B_2H_6 covers 180°. The path shown is consistent with the θ_c torsional oscillation of B_2H_6 being so strongly favored over θ_b. The 1:2 gear ratio stems from the axial symmetry of the HCl in combination with the electronic distribution and central square geometry of diborane in the ac plane.

Calculations for diborane have given[17] net charges of $+0.118$ on the borons, $+0.011$ on the bridge protons (H_b), and -0.065 on the terminal protons (H_t). The equilibrium linear configuration of the dimer can be attributed to the net attraction of the positive H in HCl to the two negative H_t's in a terminal BH_2 group, as shown at the top of Fig. 2. Also the potential surface probably has a secondary minimum at the T-shaped configuration in which the HCl is perpendicular to the BH_2B bridge, with the negative Cl end attracted to the positive charges on the borons and H_b's. This configuration, the third in Fig. 2, is then the transition state.

The tunneling postulated for B_2H_6–HCl is somewhat like that found for the "hockey-stick" N_2–H_2O complex[8] N–N···H–O–H_{bent}. The latter however has two pairs of separately interchangeable nuclei and four distinct frameworks. Both pairs of nuclei tunnel and there appears to be appreciable coupling between their motions because each of the two splittings observed can be reduced appreciably by isotopic monosubstitution of the other species. The B_2H_6–HCl differs in having only two distinct frameworks, with four pairs of simultaneously interchanged nuclei, and a tunneling path which couples the otherwise undetected reorientation of the HCl to that of the B_2H_6. If the motions of HCl were not strongly coupled to those of B_2H_6 in the tunneling species, substitution of D for H would not suppress the tunneling in $^{11}B_2H_6$–DCl.

If B_2H_6–HCl is linear, tunneling would not change the dipole moment of the dimer and transitions between tunneling states would not be allowed. Thereby each "floppy" tunneling state would have its own series of semirigid rotor transitions and rotational constants, as found. The tunneling splittings are not observed but several properties dependent on the nuclear spin statistics are affected by the tunneling, such as averaging the boron quadrupole interaction and partitioning its hfs between the A_1 and A_2 transitions. Analysis of such effects could enable one to assign more confidently

the ground torsional state but it was discouraged by the complexity and incomplete resolution of the hfs. Near the beginning of the Results section we noted that corresponding transitions of the A_1 and A_2 states were of the same intensity. The relative intensities are governed by the ratio of symmetric and antisymmetric nuclear spin functions[12] for the complex, which is 528/496 and too close to unity to call.

There are some interesting systematics in the rotational constants for the different states and species. D_J is about twice as large (10 kHz) for the A_2 than for the A_1 tunneling state, and the sixth-order constant (H) is required to fit the transitions of the A_2 state but not of the A_1. This leads us to suggest that the A_1 state is the ground vibrational state and A_2 the excited tunneling state. Moreover, centrifugal distortion of the lightest complex 10,10–H35 is very large compared to the other two tunnelers. The three nontunneling HCl species have very similar D_J and H values, which are comparable with those of the A_2 states suggesting they undergo large amplitude torsions comparable to those of the tunneling species. The two DCl species are considerably different, with both D_J and H quite small. D_{JK} for the tunneling and nontunneling HCl species is enormous and negative, -3.3 MHz, while for the DCl case it is a tenth of that, although still negative.

The torsional amplitudes γ obtained for the H/DCl from the $K=0$ hfs are given in Table VIII. They are notable for their constancy, those for HCl being 26.3° and DCl, 22.5°. The γ's for the tunneling A_2 states are consistently slightly larger (0.05°) than for the A_1, but there is no significant difference apparent between the tunneling and nontunneling states, which seems surprising. The difference between γ for the HCl and DCl species is that expected for a mass effect. In this event[15]

$$(\gamma_{\mathrm{HCl}}/\gamma_{\mathrm{DCl}}) \simeq [I_o(\mathrm{DCl})/I_o(\mathrm{HCl})]^{1/4}. \qquad (14)$$

The observed ratio of γ's is 1.17 while that of $I_o^{1/4}$ is 1.18. The γ's found by fitting the $K = \pm 1$ hfs (Table IX) agree within their limited accuracy with those from $K=0$.

Moreover there does appear to be coupling between the torsional oscillations of the H/DCl and those of B_2H_6. This is evident in the $(I_c - I_b)$ value for 11,11–D35 of 1.947 μÅ^2 compared with the values of 1.65 to 1.78 for 11,11–H35 and 10,11–H35, in Table X. Application of Eq. (11) to these data shows θ_c is 9° in the complex with DCl where $\gamma = 22.5°$ while θ_c is 10° in the complexes with HCl where γ is 26.3°.

An interesting question is "Why does the B_2H_6–HCl complex tunnel but not the B_2H_6–HF?" Lacking a potential surface, we are limited to some qualitative observations. A basic factor is probably the greater interaction energy between B_2H_6 and the HF. The well depth ϵ for the HF complex[2] is about 540 cm^{-1}. That for the HCl complex is obscured by the sensitivity of the centrifugal distortion to isotopic species and tunneling state (Table VIII). But it is clearly shallower, probably in the range 150–250 cm^{-1}. Support for this view is evident in the ground state tunneling splitting given by Schuder *et al.*[18] for $(HF)_2$ and $(HCl)_2$. That for the HCl dimer is in the 8–18 cm^{-1} range, while that of Klemperer's group[3] for the HF dimer is only 0.66 cm^{-1}.

Size and shape differences of the HF compared with HCl are also likely to be important. The HF is smaller and the H protrudes more sharply from the F, enabling it to fit more tightly with the terminal BH_2 group and making it harder for the B_2H_6 to reorient. Support for this is found by analysis of $(I_c - I_b)$ for B_2H_6–HF using Eq. (11). An earlier analysis assumed the torsional oscillations of B_2H_6 in the complex with HF to be isotropic,[2] giving $\theta_b \equiv \theta_c = 13.5°$. However, the results in Table XI make this questionable. Taking θ_b to be zero in B_2H_6–HF we find θ_c to be only 4.3° for this complex. Nonetheless the average torsional amplitude of HF is very close to that of HCl, 27° compared to 26.3°.

Although the tunneling path proposed for B_2H_6–HCl is most likely the simplest consistent with experiment, there are some variations that should be mentioned. They differ by assuming that the equilibrium configuration of the complex is bent by a small angle θ_c in the *ac* plane. The tunneling then inverts the bend coincident with reorientation of the B_2H_6 by $(180–2\theta_c)°$. Also the HCl can take either the short road, inversion, or the long, reorientation by $(360–2\theta_c)°$ counter to that of B_2H_6. Further work is needed to better map the tunneling path.

ACKNOWLEDGMENTS

Our work was supported in part by the National Science Foundation under Grant No. CHE 88-20359. Also, acknowledgment is made to the donors of the Petroleum Research Fund, administered by the American Chemical Society, for partial support of this research.

[1] R. F. W. Bader, S. G. Anderson, and A. J. Duke, J. Am. Chem. Soc. **101**, 1389 (1979); J. L. Duncan and J. Harper, Mol. Phys. **51**, 371 (1984).
[2] H. S. Gutowsky, T. Emilsson, J. D. Keen, T. D. Klots, and C. Chuang, J. Chem. Phys. **85**, 683 (1986).
[3] T. R. Dyke, B. J. Howard, W. Klemperer, J. Chem. Phys. **56**, 2442 (1972); **81**, 5417 (1984).
[4] J. A. Odutola, T. A. Hu, D. Prinslow, and T. R. Dyke, J. Chem. Phys. **88**, 5352 (1988); L. H. Coudert, F. J. Lovas, R. D. Suenram, and J. T. Hougen, *ibid.* **87**, 6290 (1987).
[5] D. D. Nelson, Jr., G. T. Fraser, and W. Klemperer, J. Chem. Phys. **83**, 945 (1985).
[6] H. S. Gutowsky, J. Chen, P. J. Hajduk, and R. S. Ruoff, J. Phys. Chem. **94**, 7774 (1990).
[7] G. T. Fraser, R. D. Suenram, F. J. Lovas, A. S. Pine, J. T. Hougen, W. J. Lafferty, and J. S. Muenter, J. Chem. Phys. **89**, 6028 (1988).
[8] H. O. Leung, M. D. Marshall, R. D. Suenram, and F. J. Lovas, J. Chem. Phys. **90**, 700 (1989).
[9] T. J. Balle and W. H. Flygare, Rev. Sci. Instrum. **52**, 33 (1981); E. J. Campbell, W. G. Read, and J. A. Shea, Chem. Phys. Lett. **94**, 69 (1983).
[10] C. Chuang, C. J. Hawley, T. Emilsson, and H. S. Gutowsky, Rev. Sci. Instrum. **61**, 1629 (1990).
[11] F. DeLucia, P. Helminger, and W. Gordy, Phys. Rev. A **3**, 1848 (1971); E. W. Kaiser, J. Chem. Phys. **53**, 1686 (1970).
[12] C. H. Townes and A. L. Schawlow, *Microwave Spectroscopy* (McGraw-Hill, New York, 1955), Chaps. 3 and 4.
[13] K. R. Symon, *Mechanics* (Addison-Wesley, Reading, MA, 1971), p. 225.
[14] W. G. Read, E. J. Campbell, and G. Henderson, J. Chem. Phys. **78**, 3501 (1983).
[15] M. R. Keenan, L. W. Buxton, E. J. Campbell, A. C. Legon, and W. H. Flygare, J. Chem. Phys. **74**, 2133 (1981).
[16] W. Gordy and R. L. Cook, *Microwave Molecular Spectra*, 3rd ed. (Wiley, New York, 1984), Chap. XIII.
[17] N. N. Greenwood, in *Comprehensive Inorganic Chemistry*, edited by A. F. Trotman-Dickenson (Pergamon, Oxford, 1973), Vol. I, Chap. 11, p. 665.
[18] M. D. Schuder, C. M. Lovejoy, D. D. Nelson, Jr., and D. J. Nesbitt, J. Chem. Phys. **91**, 4418 (1989).